



Energy Dissipation in Hilbert Envelopes on Motion Waveforms Detected in Vibrating Dynamical Systems: An Axiomatic Approach

James F. Peters^{1*}, Tharaka U. Liyanage²

Abstract

This paper introduces an axiomatic approach in the theory of energy dissipation in Hilbert envelopes on motion waveforms emanating from various vibrating dynamical systems. A Hilbert envelope is a curve tangent to peak points on a motion waveform. The basic approach is to compare non-modulated vs. modulated waveforms in measuring energy loss during the vibratory motion $m(t)$ at time t of a moving object such as a walker, runner, biker or the action of any spring system recorded in a video. Modulation of $m(t)$ is achieved by using Mersenne primes to adjust the frequency ω in the Fourier transform $m(t)e^{\pm j2\pi\omega t}$ on motion waveform $m(t)$, where the frequency ω is a Mersenne prime. Expenditure of energy $E_{m(t)}$ by a system is measured in terms of the area bounded by the motion $m(t)$ waveform at time t . Energy dissipation is measured in terms of the difference between modulated and non-modulated $m(t)$.

Keywords: Dissipation, Energy, Frequency, Hilbert envelope, Mersenne prime, Motion waveform, Vibrating Dynamical System, Video Frames

2020 AMS: 74H80, 76F20, 93A05

¹ Department of Electrical & Computer Engineerig, University of Manitoba, Winnipeg, Manitoba, R3T 5V6 and Department of Mathematics, Adiyaman University, Adiyaman, 02040 Türkiye, James.Peters3@umanitoba.ca, ORCID: 0000-0002-1026-4638

² Department of Electrical & Computer Engineerig, University of Manitoba, Winnipeg, Manitoba, R3T 5V6, uswattat@myumanitoba.ca, ORCID: 0009-0003-9521-4393

*Corresponding author

Received: 14 September 2024, **Accepted:** 16 November 2024, **Available online:** 12 December 2024

How to cite this article: J.F. Peters, T.U. Liyanage, *Energy Dissipation in Hilbert Envelopes on Motion Waveforms Detected in Sequences of Video Frames*, Commun. Adv. Math. Sci., 7(4) (2024), 178-186.

1. Introduction

Dynamical system vibrations appear as varying oscillations in motion waveforms [1, 2]. The focus in this paper is on the detection of energy dissipation that commonly occurs in vibrating dynamical systems. For a motion waveform $m(t)$ at time t , the measure of motion dissipated energy is a mapping $E_{diss} : \mathbb{R} \times \mathbb{R} \rightarrow \mathbb{R}$ defined in terms of the difference between non-modulated energy $E_{nmod}(t)$ and modulated energy $E_{mod}(t)$, i.e.,

$$\begin{aligned} E_{diss}(E_{nmod}(t), E_{mod}(t)) &= |E_{nmod}(t) - E_{mod}(t)| \\ &= |\text{non-modulated } E_m(t) - \text{modulated } E_m(t)| \end{aligned}$$

at time t of a vibratory dynamical system. In this work, two forms of motion waveform energy are considered, namely, non-modulated (non-smoothing) $m(t)$ and modulated (smoothing) $m(t)$ that results from the product of $m(t)$ and the exponential

$e^{\pm j2\pi\omega t}$ introduced by Euler [3]. A formidable source of waveform energy measurement results from the Fourier transform $m(t)e^{\pm j2\pi\omega t}$ [4](see, e.g., [5]).

A non-modulated form of waveform energy $E_m(t)$ is associated with the planar area bounded by motion curve beginning at instant t_0 and ending instant t_1 , namely, $E_m(t) = \int_{t_0}^{t_1} |m(t)|^2 dt$. In other words, system energy is identified with system waveform area, instead of the more usual energy graph [6]. Modulated system energy is measured using $E_{mod}(t) = \int_{t_0}^{t_1} |m(t)e^{\pm j2\pi\omega t}|^2 dt$.

An application of the proposed approach in measuring energy dissipation is given in terms of the Hilbert envelope on the peak points on waveforms derived from the up-and-down movements of the up-and-down movements of a walker, runner or biker recorded in a sequence of video frames. An important finding in this paper is the effective use of Mersenne primes to adjust the frequency ω of the Euler exponential to achieve waveform modulation with minimal energy dissipation (in the uniform waveform case (see Conjecture 1.i). This usage of Mersenne primes [7] of the form $2^p - 1$ (p , a prime) in modulating motion waveforms first appeared in [8]. We prove that waveform energy is a characteristic, which maps to the complex plane (See Theorem 2.10. This result extends the waveform energy results in [9], [10]) as well as in [11, 12, 13].

Symbol	Meaning
2^A	Collection of subsets of a nonempty set A
$A_i \in 2^A$	Subset A_i that is a member of 2^A
\mathbb{C}	Complex plane
t	Clock tick
$e^{j\omega t}$	$\cos(\omega t) + j\sin(\omega t)$ [3]
M	Mersenne prime
ω	Waveform Oscillation Frequency
$E_m(t)$	Energy of motion waveform $m(t)$
E_{diss}	Energy dissipation
$\varphi_t : 2^A \rightarrow \mathbb{C}$	φ maps 2^A to complex plane \mathbb{C} at time t
$\varphi_t(A_i \in 2^A) \in \mathbb{C}$	Characteristic of $\varphi(A_i \in 2^A) \in \mathbb{C}$ at time t .

Table 1.1. Principal Symbols Used in this Paper

2. Preliminaries

Highly oscillatory, non-periodic waveforms provide a portrait of vibrating systems behavior. Energy dissipation (decay) is a common characteristic of every vibrating dynamical system. Included in this paper is an axiomatic basis for measuring this characteristic of dynamical systems. A **characteristic** is a mapping $\varphi_t : A_i \rightarrow \mathbb{C}$, which maps a subsystem A_i in a system A to a point in the complex plane \mathbb{C} .

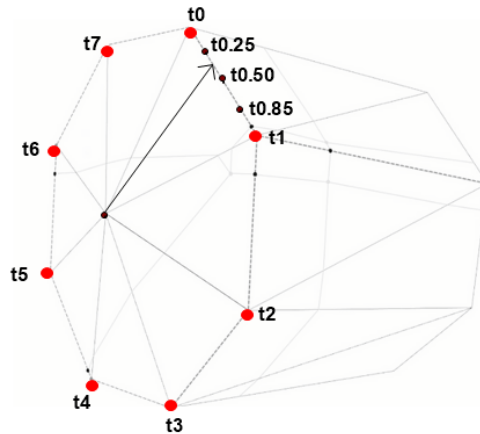


Figure 2.1. Morse instants clock

Definition 2.1. (System)

A **system** A is a collection of interconnected components (subsystems $A_i \in 2^A$) with input-output relationships.

Definition 2.2. (Dynamical System)

A dynamical system is a time-constrained, changing physical system.

Definition 2.3. (Dynamical System Output Waveform)

The output of a dynamical system is a time-constrained sequence of discrete values.

It has been observed that the theory of dynamical systems is a major mathematical discipline closely aligned with many areas of mathematics [14]. Energy dissipation is considered in many contexts such as heating, liquid (viscosity) and water-wave scattering. In this work, the focus is on energy decay represented by the difference between the energy of non-smooth (non-modulated) and smooth (modulated) motion waveforms. A motion waveform is a graphical portrait of the radiation emitted by moving system (e.g., walker, runner, biker) with oscillatory output.

Axiom 1. (Instants Clock)

Every system has its own instants clock, which is a cyclic mechanism that is a simple closed curve with an instant hand with one end of the instant hand at the centroid of the cycle and the other end tangent to a curve point indicating an elapsed time in the motion of a vibrating system. A clock tick occurs at every instant that a system changes its state.

Remark 2.4. (What Euler tells us about time)

On an instants clock, every reading $t \in (\mathbb{C})$, a point $t = a + jb, a, b \in \mathbb{R}$ in the complex plane. For example, $t_{0.25} = 0.25 + j0 = 0.25$ in Fig. 2.1. The Morse instants clock is also called a homographic clock [15], since the tip of an instant clock t -hand moves on the circumference of a circle, where t is a complex number [15]. For t at the tip of a vector with radius $r = 1$, angle θ and $a = \cos\theta, b = \sin\theta$ in the complex plane, then

$$t = a + jb = \cos\theta + j\sin\theta = e^{j\theta}.$$

An instant of time viewed as an exponential is inspired by Euler [3].

Example 2.5. A sample Morse instants clock is shown in Fig. 2.1. The clock hand points to the elapsed time in the interval $(t_{0.25} \leq t \leq t_{0.25})$ in milliseconds (ms) after a system has begun vibrating. The clock face is a polyhedral surface in a Morse-Smale surface in a convex polyhedron in 3D Euclidean space. A Morse-Smale polyhedron is an example of a mechanical shape descriptor ideally suited as clock model because of its underlying piecewise smooth geometry. This form of an instants clock has been chosen to emphasize that the elapsed time t_k is a real number in an instants interval $[t_0, t_k] \in \mathbb{C}^2$ in which t_k is indeterminate. From a planar perspective, the proximity of sets of instants clock times is related to results given for computational proximity in the digital plane [16]. In this example, the instant hand is pointing to an elapsed time between $t_{0.25}$ ms and $t_{0.50}$ ms.

Definition 2.6. (Clocked Characteristic of a subsystem)

The clocked characteristic of a subsystem A_i of a system A at time $\varphi_t(A_i)$ is a mapping $\varphi_t : A_i \in 2^A \rightarrow \mathbb{C}$ defined by $\varphi_t(A_i) = a + bj \in \mathbb{C}, a, b \in \mathbb{R}, j = \sqrt{-1}, \varphi_t(A_i) \in \mathbb{C}$.

Axiom 2. (Subsystem Motion Characteristic)

Let $A_i \in 2^A$ (subsystem A_i in the collection of subsystems 2^A in system A) that emits changing radiation due to system movements (motion) and let t be a clock tick. The motion characteristic of subsystem motion $A_i \in 2^A$ is a mapping $m_t : A_i \rightarrow \mathbb{C}$ defined by

$$m_t(A_i) = a + bj \in \mathbb{C}, a, b \in \mathbb{R}, j = \sqrt{-1}, t \in \mathbb{R}.$$

i.e., a subsystem A_i motion characteristic of a system A is a mapping $m_t(A_i \in 2^A) \in \mathbb{C}$ at time t .

Remark 2.7. For the motion characteristic, we write $dm(t)$ when it is understood that motion is on a subset $A_i \in 2^A$ in a dynamical system A . Axiom 2 is consistent with the view [17] of the characteristic vector field, represented here with a planer characteristic vector field ξ of a dynamical system with points $p(x, y, t) \in \xi$ that has positive complex characteristic coordinates at clock tick (time) t such that

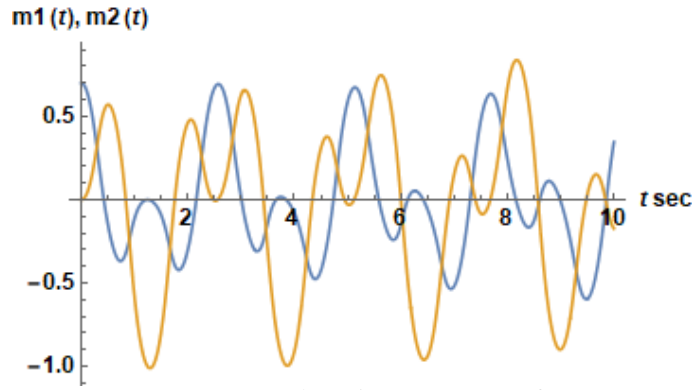


Figure 2.2. Sample spring system waveforms

$$\varphi_t(A_i \in 2^A) = p \in \xi = (a - jb) \frac{\partial \xi}{\partial x} + (a - jb) \frac{\partial \xi}{\partial y} + (a - jb) \frac{\partial \xi}{\partial t}, a, b \in \mathbb{R}.$$

The 1-1 correspondence between every point p having coordinates in the Euclidean plane and points in the complex plane is lucidly introduced by D. Hilbert and S. Cohn-Vossen [18, §38, 263-265]. For an introduction to characteristic groups, see [19],[20],[21].

Example 2.8. Spring system vibration

A pair of sample sinusoidal waveforms emitted by an expanding and contracting spring system is shown in Fig. 2.2.

Vibrating system waveform $m(t)$ modulation (smoothing) is achieved by adjusting the frequency ω in an Euler exponential $e^{\pm j2\pi\omega t}$, which is used in oscillatory waveform curve smoothing. It has been found that Mersenne primes provide an effective means an effective means of adjusting the frequency ω . It has been observed by G.W. Hill [22] that Mersenne primes $M_p = 2^p - 1 = 3, 7, 31, \dots$ for prime $p = 2, 3, 5, \dots$ are useful in estimating variability as well as in estimating average values in sequences of discrete values.

Axiom 3. (Waveform Energy)

A measure of dynamical system energy is the area of a finite planar region bounded by system waveform $m(t)$ curve at time t , defined by

$$E_m(t) = \int_{t_0}^{t_1} |m(t)|^2 dt.$$

Lemma 2.9. Dynamical system energy is time-constrained and is always limited.

Proof. Let E_m be the energy of a dynamical system, defined in Axiom 3. From Axiom 3, system energy always occurs in a bounded temporal interval $[t_0, t_1]$. Hence, E_m is time constrained. From Axiom 1, the length of a system waveform is finite, since, from Axiom 3, system duration is finite. From Axiom 3, system energy is derived from the area of a finite, bounded region. Consequently, system energy is always finite. \square

Theorem 2.10. If X is a dynamical system with waveform $m(t)$ at time t and which changes with every clock tick, then observe

- 1° System waveform characteristic values are in the complex plane.
- 2° System energy varies with every clock tick.
- 3° System radiation characteristics are finite.
- 4° All system characteristics map to the complex plane.
- 5° Waveform energy decay is a characteristic, which maps to \mathbb{C} .

Proof.

- 1° From Def. 2.6, a system characteristic is a mapping from a subsystem to the complex plane at time t , From Axiom 2, every waveform motion characteristic $m(t) \in \mathbb{C}$ at time t , which is the desired result.

- 2^o From Lemma 2.9, system energy is time-constrained and always occurs in a bounded temporal interval. From Axiom 1, there is a new clock tick at every instant in time t ms. From Axiom 3, system energy varies with every clock tick.
- 3^o From Axiom 1, all system radiation characteristics are finite, since system duration is finite.
- 4^o From Axiom 2, every system A characteristic is a mapping from a subsystem $A_i \in 2^A$ to the complex plane, which is the desired result.
- 5^o From the proof of step 4, the desired result follows.

□

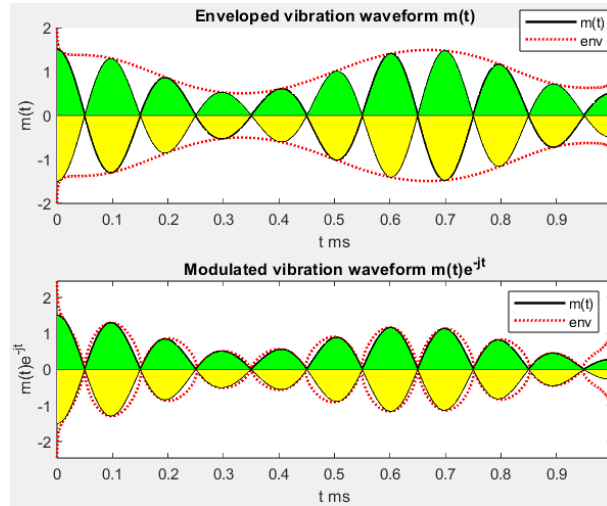


Figure 2.3. Hilbert envelope on modulated vibration waveform.

To obtain an approximation of system energy, a system waveform is represented by a continuous curve defined by a Hilbert envelope [23] tangent to waveform peak points, forming what known as Hilbert lobes.

A **Hilbert envelope** (denoted by H_{env}) is a curve that is tangent to the peak points on a waveform [24, §18.4, p. 132]. A **Hilbert envelope lobe** (denoted by $H_{envlobe}$) is a tiny bounded planar region attached to single waveform peak point on a waveform envelope, defined by

$$H_{env} = \sqrt{m(t)^2 + (-m(t))^2} [23]$$

The energy represented by a lobe $H_{envlobe}$ area of a tiny planar region attached to an oscillatory motion waveform $m(t)$ is defined by

$$H_{envlobe} = \int_a^b |m(t)|^2 dt$$

It is lobe area that provides a measure of the energy represented by a waveform segment.

The modulated vibration waveform $m(t)$ in Fig. 2.3 varies with lower peak points than the original motion waveform, depending on the choice of Mersenne prime frequency. To minimize energy loss due to modulation, a Mersenne prime is chosen for the frequency ω in an Euler exponential in $m(t)e^{\pm j\omega t}$ to obtain

result.1^o Modulated system waveform $m(t)$ is smoother for a particular Mersenne prime frequency (i.e., the waveform oscillations are more uniform).

result.2^o Modulated system energy loss is minimal, for a particular Mersenne prime frequency.

3. Application: Modulating System Waveform with Minimal Energy Dissipation

In this section, we illustrate how Mersenne primes can be used effectively to obtain the following results:

M \rightarrow ω -1^o Usage of a M-prime as the frequency in the Euler exponential in

$$m(t)e^{\pm j\omega M t}$$

reduces motion $m(t)$ waveform motion energy.

$M \rightarrow \omega^{-2}$ Energy dissipation varies in modulated vs. non-modulated waveforms for different choices of frequency M in $e^{\pm j\omega M t}$, depending on whether a waveform has uniformly or non-uniformly varying cycles around the origin.

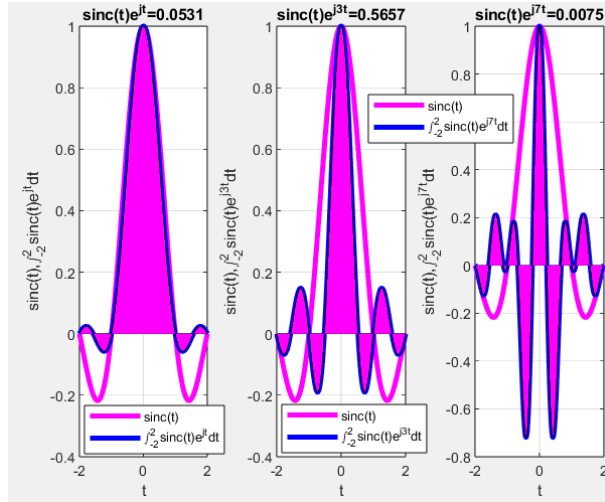


Figure 3.1. 3 forms of $m(t)e^{j\omega t}$

Conjecture 1. The choice of a Mersenne prime $M \leq 31$ will always result in lower motion waveform peak values using M as the frequency in the Euler exponential to achieve waveform modulation and minimal energy dissipation.

There are two cases to consider: [Partial Picture Proof]

Case(i) Assume $m(t)$ waveform uniformly fluctuates and frequency $\omega = M = 1$ results in the lowest energy loss

Proof. Partial picture proof: Recall that $e^{j\omega t} = \cos\omega t + j\sin\omega t$, where $m(t)e^{j\omega t}$ forces the oscillation in a motion waveform to increase. Let $m(t) = \text{sinc}(t)$, introduced in 1822 by Fourier [4]. Then $m(t)$ oscillates uniformly on either side of the origin (see sample plot of $\text{sinc}(t)$ in Fig. 3.1). The area of $m(t) = \int_{-k}^k \text{sinc}(t)e^{j\omega t} dt$, $\omega \geq 1$ is always less than the area $\int_{-k}^k \text{sinc}(t)dt$. That is, $e^{j\omega t}$ partitions each $m(t)$ cycle into regions with smaller areas whose total area is less than the total area $\int_{-k}^k \text{sinc}(t)dt$. With $\omega = M = 1$, the modulated waveform energy is closest to non-modulated waveform energy, which is the desired result. \square

Case(ii) Let $m(t)$ be a non-uniform waveform. We make the unproved claim that the choice of $\omega = M$, varies, i.e., M is not always 1.

Example 3.1. Sample Energy Dissipation: Non-uniform waveform Case

Let $m(t) = \text{sinc}(t)$, with cycles that vary uniformly relative to the origin. This is the case in Fig. 3.1. The result for 3 choices of $M \in \{1, 3, 7\}$ are shown in the plots in Fig. 3.1. This leads to the following energy dissipation levels:

$$E_{m(t)} = 0.9028 \text{ non-modulated waveform energy}$$

$$E_{m(t)e^{jt}} = 0.1503 \text{ } M = 1, \text{ modulated waveform energy loss}$$

$$E_{m(t)e^{j3t}} = 0.3371 \text{ } M = 3, \text{ modulated waveform energy loss}$$

$$E_{m(t)e^{j7t}} = 0.8954 \text{ } M = 7, \text{ modulated waveform energy loss}$$

$$E_{m(t)e^{j31t}} = 0.9021 \text{ } M = 31, \text{ modulated waveform energy loss}$$

The $\omega = M = 31$ case is not shown in Fig. 3.1.

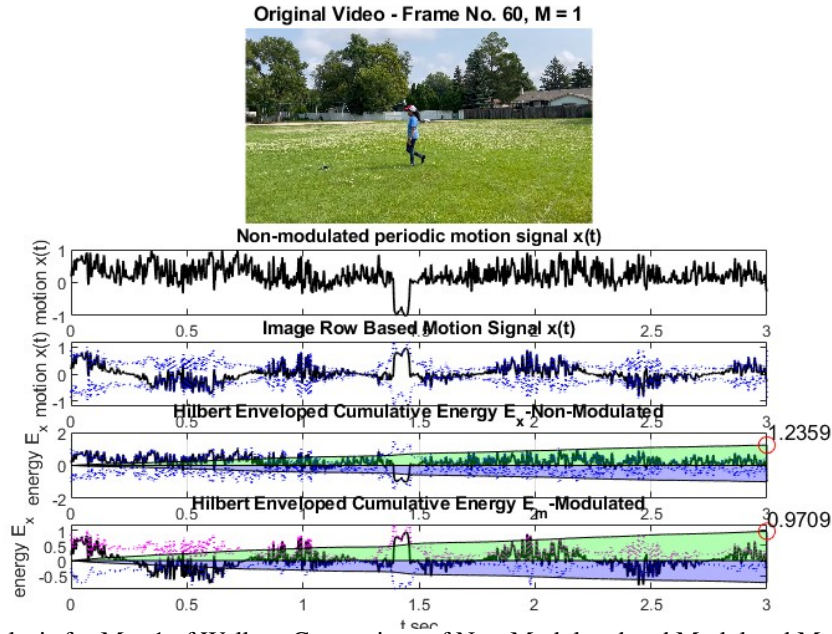


Figure 3.2. Energy Analysis for $M = 1$ of Walker: Comparison of Non-Modulated and Modulated Motion Signals of Frame = 60

Evidence of the correctness of our Conjecture for the non-uniform waveform case in the choice of the Mersenne prime to achieve minimal energy dissipation can be seen in the following two examples.

Example 3.2. Sample Energy Dissipation for a walker waveform

A sample collection of non-modulated and modulated waveforms for a walker for $M = 1$ is shown in Fig. 3.2. In Table 2, $M = 1$ for the exponential frequency of a modulated waveform results in the lowest energy dissipation.

However, if consider the choice of M for the modulation frequency for a biker, this choice differs from the choice of $M = 1$ in Example 3.2.

M	Non-Modulated Energy (E _x)	Modulated Energy (E _m)	Energy Dissipation Percentage
1	1.2359	0.9709	21.44%
3	1.2359	0.9222	25.38%
7	1.2359	0.9559	22.65%
31	1.2359	0.9166	25.83%

Table 3.1. Energy Dissipation for Walking

M	Non-Modulated Energy (E _x)	Modulated Energy (E _m)	Energy Dissipation Percentage
1	0.9635	0.6317	34.43%
3	0.9635	0.6729	30.16%
7	0.9635	0.6561	31.90%
31	0.9635	0.6396	33.61%

Table 3.2. Energy Dissipation for Biking

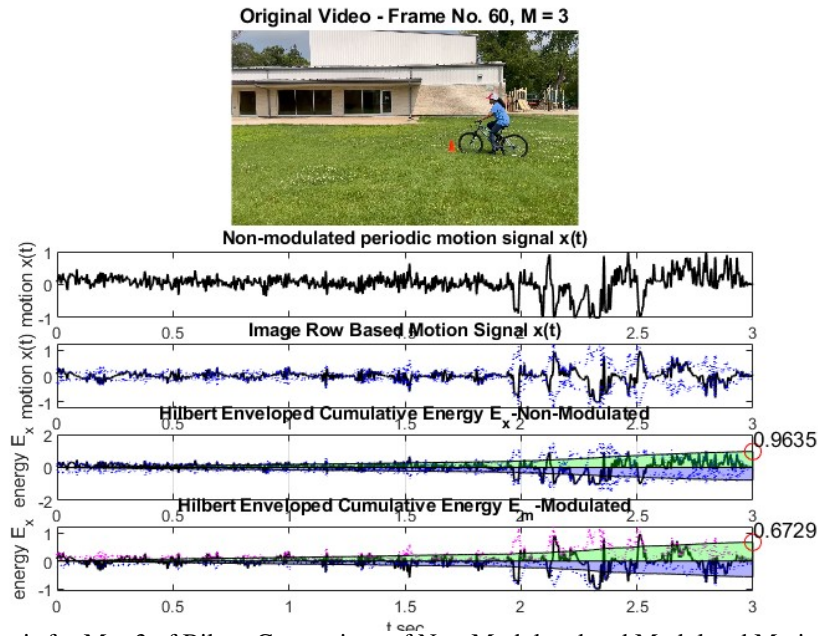


Figure 3.3. Energy Analysis for $M = 3$ of Biker: Comparison of Non-Modulated and Modulated Motion Signals of Frame = 60

Example 3.3. Sample Energy Dissipation for a biker waveform

A sample collection of non-modulated and modulated waveforms for a biker for $M = 3$ is shown in Fig. 3.3. In Table 3, $M = 3$ for the exponential frequency of a modulated waveform results in the lowest energy dissipation.

4. Conclusion

This paper focuses on the frequency characteristic in modulating dynamical system waveforms. The appropriate choice of Mersenne prime M as the frequency ω for the Euler exponential $e^{j\omega t} \rightarrow e^{jMt}$ is considered in modulating a dynamical system waveform to obtain a smoother waveform and achieve minimal energy dissipation. It has been found that $M = 1$ is the best choice for waveforms whose cycles vary uniformly about the origin. Choice of $M \in \{1, 3, 7, 31\}$ for the non-uniform waveforms varies, depending on how extreme the lack of self-similarity present in waveforms that vary in a chaotic fashion on either side of the origin. The appropriate choice of M in modulating a non-uniform waveform is an open problem.

Article Information

Acknowledgements: The authors extend their profound thanks to the reviewers, who make very helpful suggestions. We also wish to thank Tane Vergili for sharing her insights concerning the underlying topology and proximity space theory in this paper. In addition, we extend our thanks to Andrzej Skowron, Mirosław Pawlak, Divagar Vakeesan, Enze Cui, Younes Shokoohi, William Hankley, Brent Clark and Sheela Ramanna for sharing their insights concerning time-constrained dynamical systems. In some ways, this paper is a partial answer to the question 'How [temporally] Near?' put forward in 2002 [25].

Author’s contributions: All authors contributed equally to the writing of this paper. All authors read and approved the final manuscript.

Conflict of Interest Disclosure: No potential conflict of interest was declared by the authors.

Copyright Statement: Authors own the copyright of their work published in the journal and their work is published under the CC BY-NC 4.0 license.

Supporting/Supporting Organizations: This research has been supported by the Natural Sciences & Engineering Research Council of Canada (NSERC) discovery grant 185986 and Instituto Nazionale di Alta Matematica (INdAM) Francesco Severi, Gruppo Nazionale per le Strutture Algebriche, Geometriche e Loro Applicazioni grant 9 920160 000362, n.prot U 2016/000036 and Scientific and Technological Research Council of Turkey (TÜBİTAK) Scientific Human Resources Development (BİDEB) under grant no: 2221-1059B211301223.

Ethical Approval and Participant Consent: It is declared that during the preparation process of this study, scientific and ethical principles were followed and all the studies benefited from are stated in the bibliography.

Plagiarism Statement: This article was scanned by the plagiarism program.

References

- [1] R. De Leo, J. A. Yorke, *Streams and graphs of dynamical systems*, Qual.Theory Dyn. Syst., **24** (2024), 53 pages.
- [2] M. Feldman, *Hilbert Transform Applications in Mechanical Vibration*, John Wiley and Sons, Ltd., N.Y., 2011.
- [3] L. Euler, *Introductio in Analysin Infinitorum*, Sociedad Andaluza de Educacion Matematica Thales, Springer, New York, 1988.
- [4] J. B. J. Fourier, *Theorie Analytique de la Chaleur*, Analytic Theory of Heat, Cambridge University Press, Cambridge, U.K., 2009.
- [5] B. Peng, X. Wei, B. Deng, H. Chen, Z. Liu, X. Li, *A sinusoidal frequency modulation fourier transform for radar-based vehicle vibration estimation*, IEEE Transactions on Instrumentation and Measurement, **63**(9) (2014), 2188–2199.
- [6] J. Kok, N. K. Sudev, K. P. Chitha, U. Mary, *Jaco-type graphs and black energy dissipation*, Adv. Pure Appl. Math., **8**(2) (2027), 141–152.
- [7] M. Mersenne, *Cogitata Physico-Mathematica*, Sumptibus Antonii Bertier, Paris, 1644.
- [8] T. U. Liyanage, *Detecting Energy Dissipation in Modulated vs. Non-Modulated MotionWaveforms Emanating from Vibrating Systems Recorded in Videos*, M.Sc. Thesis, University of Manitoba, 2024.
- [9] S. Tiwari, J. F. Peters, *Proximal groups: extension of topological groups. application in the concise representation of Hilbert envelopes on oscillatory motion waveforms*, Comm. Algebra, **52**(9) (2024), 3904–3914.
- [10] M. S. Haider, J. F. Peters, *Temporal proximities: self-similar temporally close shapes*, Chaos, Solitons and Fractals, **151** (2021), 10 pages.
- [11] J. F. Peters, T. Vergili, *Good coverings of proximal Alexandrov spaces. Path cycles in the extension of the Mitsuishi-Yamaguchi good covering and Jordan curve theorems*, Appl. Gen. Topol., **24**(1) (2023), 25–45.
- [12] E. Ozkan, B. Kuloglu, J. F. Peters, *k-Narayana sequence self-similarity. Flip graph views of k-Narayana self-similarity*, Chaos, Solitons and Fractals, **153**(2) (2021), 11 pages.
- [13] E. Erdag, J. F. Peters, O. Deveci, *The Jacobsthal-Padovan-Fibonacci p-sequence and its application in the concise representation of vibrating systems with dual proximal groups*, J. Supercomput, **81** (2025), 197-220.
- [14] A. Katok, B. Hasselblatt, *Introduction to the Modern Theory of Dynamical Systems*, Encyclopedia of Mathematics and its Applications 54, Camb. Univ. Press, Cambridge, UK, 1995.
- [15] L. Hofmann, E. Kasner, *Homographic circles or clocks*, Bull. Amer. Math. Soc., **34**(4) (1928), 495–503.
- [16] J. F. Peters, *Vortex nerves and their proximities. Nerve Betti numbers and descriptive proximity*, Bull. Allahabad Math. Soc., **34**(2) (2019), 263–276.
- [17] D. E. Blair, *Contact Manifolds in Riemannian Geometry*, Springer Verlag, Berlin-Heidelberg, 1976.
- [18] D. Hilbert, S. Cohn-Vossen, *Geometry and the Imagination*, Chelsea Pub. Co., New York, 1952.
- [19] N. Tziolas, *Topics in group schemes and surfaces in positive characteristic*, Ann. Univ. Ferrara Sez. VII Sci. Mat., **70**(3) (2024), 891–954.
- [20] E. Bombieri, D. Mumford, *Enriques' classification of surfaces in char. p. III*, Invent. Math., **35** (1976), 197–232.
- [21] W. E. Lang, *Quasi-elliptic surfaces in characteristic three*, Ann. Sci. École Norm. Sup.(4), **12**(4) (1979), 473–500.
- [22] E. Hill, M. Zorn, *Open Additive Semi-Groups of Complex Numbers*, Annals of Math., **44**(3) (1943), 554–561.
- [23] A. Brandt, *Noise and Vibration Analysis. Signal Analysis and Experimental Procedures*, N.Y., U.S.A., Wiley, 2011.
- [24] F. W. King, *Hilbert Transforms*, Cambridge University Press, Cambridge, UK, 2009.
- [25] Z. Pawlak, J. F. Peters, *How Near Are Zdzisław Pawlak's Paintings?*, In: Systemy Wspomagania Decyzji, **I** (2007), 57–109.